

## DATA ARTICLE

# Local water year values for the conterminous United States

Xinyu Sun ,<sup>1\*</sup> Kendra Spence Cheruvellil <sup>1,2</sup>

<sup>1</sup>Department of Fisheries and Wildlife, Michigan State University, East Lansing, Michigan, USA; <sup>2</sup>Lyman Briggs College, Michigan State University, East Lansing, Michigan, USA

### Scientific Significance Statement

Scientists and managers use “water year” to estimate precipitation and water flow, and their impacts on ecosystems. A single water year is traditionally applied to a large geographic area (e.g., entire conterminous United States). However, this coarse approach overlooks the sometimes large regional spatial variation or asynchrony between precipitation and water fluxes at large spatial scales, both of which are increasingly more variable in many regions globally due to climate change. Our work fills this need by using widely available streamflow data and existing localized definitions of water year to develop local water year values for each of the 202 subregions across the conterminous United States. Use of these data will improve our ability to understand and predict climate change impacts on ecosystems at broad spatial scales.

### Abstract

Quantifying and predicting precipitation and water flow and their influences is challenged by the dynamic relationships between and timing of precipitation and water fluxes. To help with these challenges, scientists use “water year” to examine and predict the impacts of precipitation and relevant extreme climatic and hydrological events on ecosystems. However, traditional water year definitions used in the US lack a consideration of areal variation in climate and hydrology, which is needed when studying ecosystems at regional or national scales. We developed local water year (LWY) values that consider spatial variation using existing definitions whereby the water year begins in the month with the lowest or highest average monthly streamflow. We employed spatial interpolation to assign LWY start and end months to 202 subregions across the conterminous United States that range from 4,384 to 134,755 km<sup>2</sup>. This dataset can be linked with diverse climate, terrestrial, and aquatic data for broad-scale studies.

Precipitation plays a crucial role in shaping hydrology and ecosystems. Precipitation can be highly spatially variable, especially when considering macroscale spatial extents of

regions to continents (Mock 1996; Augustine 2010). As a result of climate change, there has been greater inter-annual variability in precipitation in many regions worldwide

\*Correspondence: [16xs6@queensu.ca](mailto:16xs6@queensu.ca); [sunxiny9@msu.edu](mailto:sunxiny9@msu.edu)

This is an open access article under the terms of the [Creative Commons Attribution](https://creativecommons.org/licenses/by/4.0/) License, which permits use, distribution and reproduction in any medium, provided the original work is properly cited.

**Associate editor:** Matthew R. V. Ross

**Data Availability Statement:** Local water year (LWY) data and metadata, as well as the code used to create LWYs, are available on the Environmental Data Initiative (EDI) Data Portal at <https://doi.org/10.6073/pasta/c27e57749f856bd24dc7c7559b9b316b>.

**Measurement(s):** Local water year. **Technology type(s):** Spatial interpolation. **Temporal range:** 1990–2018. **Frequency or sampling interval:** Single snapshot. **Spatial scale:** Conterminous United States.

(IPCC 2021), causing increased frequency and intensity of extreme climatic and hydrological events such as drought and flooding (Easterling et al. 2000; Grimm and Natori 2006; Prein et al. 2016; Kundzewicz et al. 2020). In addition, water fluxes are sometimes asynchronous with precipitation and extreme events can occur during the transition between years, complicating hydrological estimations. For example, rainfall in late fall can be retained in the soil and influence water fluxes the following spring (Pike 1964; Kamps and Heilman 2018). Despite such spatial and temporal variation and asynchronicity in precipitation, a calendar year timeframe (from January 1<sup>st</sup> to December 31<sup>st</sup>) has often been used to examine and predict the impacts of precipitation and relevant extreme climatic and hydrological events on aquatic systems.

To more accurately predict water flow, researchers adopted a “water year” that usually spans two standard calendar years. For example, the U.S. Geological Survey (USGS) water year, which was adopted a century ago, starts on October 1<sup>st</sup> and ends on September 30<sup>th</sup> of the next year (Henshaw et al. 1915). This USGS water year is applied to the whole United States and intends to account for the influence of snowfall from October to December on the next year’s streamflow (Henshaw et al. 1915). However, different regions of the United States have different timing of precipitation (including snowfall) and hydrology, as well as varying topographic patterns, all of which affect relationships between (and timing of) precipitation and water fluxes (Nicótina et al. 2008; Condon and Maxwell 2015; Torre Zaffaroni et al. 2023). These facts mean that a more localized timeframe is needed rather than applying a single water year to the macroscale.

Researchers have started to use various definitions for water year, and subsequent start/end times of that water year depend on the locations, ecosystem types, and research purposes or questions. For example, Olson et al. (2013) started their water year in April when analyzing the methane and carbon dioxide fluxes of a temperate peatland, Kamps and Heilman (2018) started their water year in September to match annual precipitation with water and carbon budgets in Central Texas, and Caruso (2000) started water years from July or October so that the low-streamflow periods in the Otago region in New Zealand could be fully captured. These (and other) studies use water years for a relatively local spatial extent (e.g., watershed or single region). However, organisms and ecological processes are influenced by multi-scale factors, from local (e.g., lake morphometry) to regional (e.g., land use) and macroscale (e.g., climate), and these factors can sometimes interact to affect ecosystems (Heffernan et al. 2014; Rose et al. 2017; LaRue et al. 2021). Thus, it is crucial to investigate and predict how ecosystems respond to environmental changes, such as precipitation variability and relevant extreme events, across multiple spatial and temporal scales. Therefore, localized water year timeframes are needed for a range of research purposes at regional to continental scales.

One challenge to creating localized water year timeframes has been limited data for variables such as snow melting time, ice-off dates, and annual gross primary productivity (e.g., Olson et al. 2013; Kamps and Heilman 2018). However, Wasko et al. (2020) proposed a climate- and hydrology-relevant local water year (LWY) timeframe that solely used streamflow data that are available for most areas globally. This LWY provides a site-specific timeframe beginning in the month with the lowest average monthly streamflow to capture the concurrent and lagged associations between precipitation and hydrology (Wasko et al. 2020). Using this localized timeframe, they predicted the timing and trends of flooding and streamflow at the global scale and demonstrated an improved accuracy of estimation compared with using a calendar year timeframe (Wasko et al. 2020).

Although a big step forward for global studies relying on water year data, these data do not completely cover the conterminous United States (CONUS), which may limit regional to CONUS-scale research. Thus, we build on their work by extending this LWY timeframe to cover the CONUS. We used recent (1990–2018) streamflow data, the same method used by Wasko et al. (2020), and a spatial interpolation method to construct a CONUS-scale LWY timeframe. In addition, given that the most appropriate definition of water year varies depending on research purposes, we applied the same process and generated a second LWY timeframe starting from the month with the highest average monthly streamflow, an approach often used in studies of low streamflow and hydrological drought (e.g., Caruso 2000; Chagas et al. 2024). To create these LWYs, we used subregions that were created based on the drainage features by the USGS (Seaber et al. 2007). This hierarchical regionalization framework divides and subdivides the United States into successively smaller hydrologic units (HUs); we used the HU4 subregion, which is the second-level classification that delineates large river basins (USGS 2024). We included 202 HU4s in the CONUS that range in area from 4,384 to 134,755 km<sup>2</sup>. These LWY data will help advance the understanding of the impacts of variability in precipitation and streamflow on inland waters at the regional and national US scales.

### Data description

This data product consists of two datasets housed on the Environmental Data Initiative (EDI) repository (<https://doi.org/10.6073/pasta/c27e57749f856bd24dc7c7559b9b316b>), as well as our R code (file name: local water year code.R). The first dataset (file name: water years 875 sites.csv) was used to develop and evaluate the LWY end month across the CONUS. This file includes the identifier from the Global Runoff Data Centre, which is the archive where we obtained streamflow data (“grdc\_no” column), end month of the LWY that begins from the month with the lowest average monthly streamflow

(“end.month.lowest” column), end month of the LWY that begins from the month with the highest average monthly streamflow (“end.month.highest” column), and locational information (longitude (“lon” column), latitude (“lat” column), altitude (“altitude” column), and the name of the river (“river” column) and station (“station” column) of each gauging site where the daily streamflow data were measured) (the process of site selection will be described in the next section). There are a total of 875 sites. When the LWY starts from the lowest-flow month, the most common LWY end month among these sites is July (228 sites), followed by August (219 sites), December (160 sites), and September (78 sites) (Figs. 1a, 2a). When the LWY starts from the highest-flow month, the most common end month is April (214 sites), followed by February (175 sites), March (145 sites), and May (134 sites) (Figs. 3a, 4a).

The second dataset (file name: hu4 water years with notes.csv) contains the LWY data for each subregion. This file includes the start (“start.month.lowest” column) and end month (“end.month.lowest” column) of the LWY that begins from the month with the lowest average monthly streamflow as well as the start (“start.month.highest” column) and end month (“end.month.highest” column) of the LWY that begins from the month with the highest average monthly streamflow for each of the 202 subregions (i.e., 4-digit Hydrologic Unit; HU4) across the CONUS (“hu4.code” column). This dataset also includes two “notes” columns (“notes.lowest” and “notes.highest”) that provide details about whether there were streamflow data in the subregion and the method we used to determine the LWY end month. There are three categories in this column: (1) *dominant\_interpolation*, which indicates that there were streamflow data and we based the end month on the single, dominant (i.e., most commonly occurring) interpolated LWY end month value in the subregion; (2) *local\_sites\_based*, which indicates that there were streamflow data and multiple LWY end month values in the subregion; therefore, end month was based on the site-specific LWY data; and (3) *ND\_interpolation*, which indicates that there were no streamflow data in the area and the end month was determined based on the dominant LWY end month value from interpolation of nearest sites. More details about the methodology can be found in Sections 2 and 3.

The results of this work are 404 LWYs, two for each subregion across the CONUS. There are spatial differences in LWY end months (Figs. 2b, 4b). For example, along the eastern and western edges of the CONUS, the LWY that begins from the month with the lowest streamflow (hereafter referred to as LWY-lowest) usually ends in July or August, except for the very southeast where it ends in April. In contrast, there is much more heterogeneity in LWY-lowest in the central United States, with November and December being the most common end months. The most common end month for LWY-lowest is August (64 subregions), followed by July

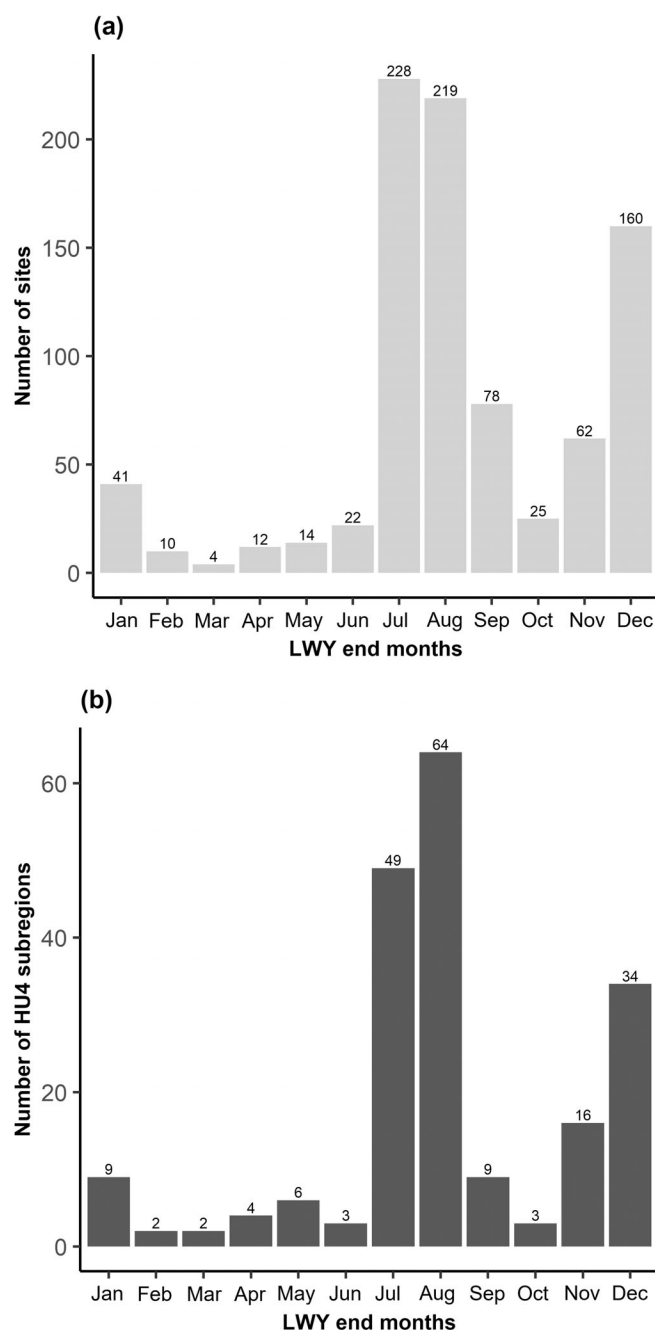


**Fig. 1.** The number of stream gauging sites (a) and subregions (b) by the end month of the local water year (LWY) that starts from the month with the lowest average monthly streamflow (LWY-lowest). The numbers above each bar indicate the number of sites (top) or subregions (bottom). Subregion = HU4 (Seaber et al. 2007). More information about HU4s can be found on the USGS website: <https://water.usgs.gov/GIS/huc.html>, last accessed September 2023.

(49 subregions), December (34 subregions), and November (16 subregions) among all subregions (Fig. 1b). When LWY starts from the highest-flow month (hereafter referred to as LWY-highest), the end months are often February and March



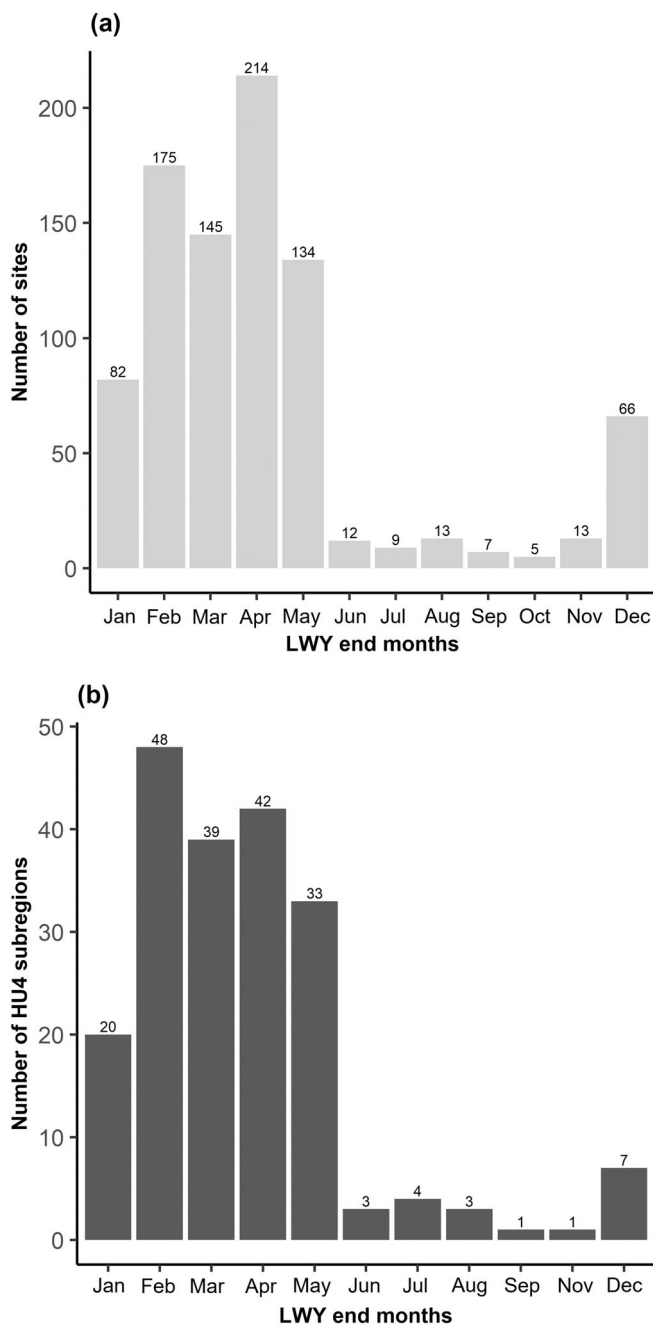


**Fig. 3.** The number of stream gauging sites (a) and subregions (b) by the end month of the local water year (LWY) that starts from the month with the highest average monthly streamflow (LWY-highest). The numbers above each bar indicate the number of sites (top) or subregions (HU4; bottom).

We computed the semivariogram, which depicts the spatial correlation between the neighboring values, using Eq. (1),

$$\gamma(h) = \frac{1}{2n} \sum_{i=1}^n [Z(x_i) - Z(x_i + h)]^2 \quad (1)$$

where  $\gamma(h)$  is the semivariogram;  $Z(x_i)$  and  $Z(x_i + h)$  are the data at locations  $x_i$  and  $x_i + h$ , respectively; and  $n$  is the number of pairs of data separated by distance  $h$  (Li and Heap 2011; Sanabria et al. 2013). Second, we fit a mathematical model to the semivariogram. The spherical function was used in our model, and we adjusted parameter values (e.g., partial sill, range, and nugget) to improve the model fit. Third, we applied this semivariogram model to interpolate the LWY-lowest end month data, by using Eqs. (2) and (3) to estimate the local data (at the unsampled location) using neighboring data,

$$Z^*(x_0) = \sum_{i=1}^n \lambda_i Z(x_i) \quad (2)$$

$$\text{var}\{Z^*(x_0) - Z(x_0)\} = \text{minimum} \quad (3)$$

where  $Z^*(x_0)$  is the estimated value at location  $x_0$ ;  $Z(x_i)$  is the data value at location  $x_i$ ; and  $\lambda_i$  is the weighting factor that is determined by minimizing the variance (Eq. 3). Finally, we overlaid the interpolated end month LWY-lowest values with subregion polygons for the CONUS to assign the LWY-lowest end month for each subregion.

The resulting 202 subregion LWY-lowest values include 156 subregions that were labeled “dominant\_interpolation” in the dataset (hu4 water year with notes.csv, “notes.lowest” column). These subregions had streamflow data and a single dominant (i.e., most commonly occurring) interpolated LWY-lowest end month in the subregion, so the end month was chosen based on the dominant value. There were 29 subregions labeled as “local\_sites\_based,” which indicates that there were streamflow data but multiple different LWY-lowest end month values in the subregion. It was difficult to determine the dominant month of these subregions based on interpolation results, thus the decision of the LWY-lowest end month of the subregion was made by checking the site-specific LWY data in each of the subregions and determining the dominant month of each subregion. For the 17 subregions labeled “ND\_interpolation,” there was no streamflow data and the month was determined solely based on interpolation results and the dominant interpolated LWY-lowest end month value.

### Local water year beginning with the highest streamflow month (local water year-highest)

For each site, we used the calculated average monthly streamflow data and compared these monthly averages to determine the month with the highest streamflow, which became the start month of a site’s LWY. When the highest-streamflow-month varied among years for a site, the start month of a site’s LWY-highest was the highest-streamflow-month with the highest frequency of occurrence. Then, following the processes described above, we applied spatial interpolation and obtained 202 subregion LWY-highest values, including 178 subregions that were labeled “dominant\_interpolation” in the dataset (hu4 water year with notes.

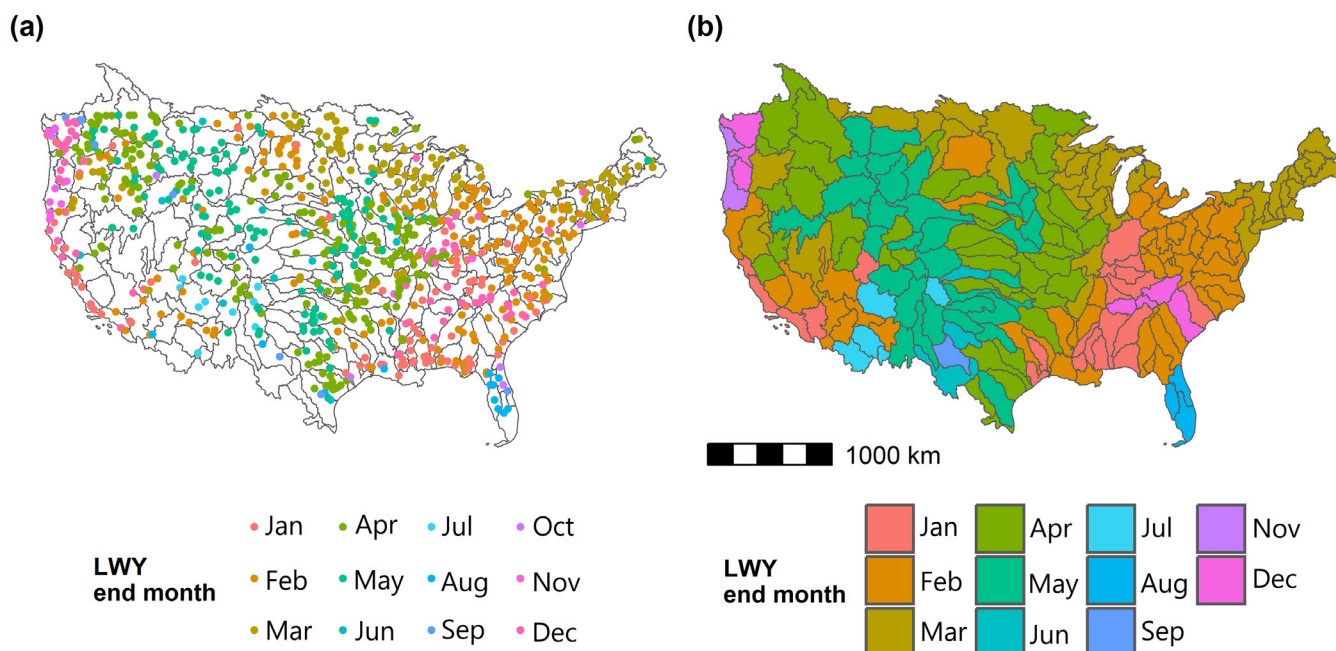


**Fig. 4.** Maps showing the LWY-highest end month of each site overlaid with subregion (HU4) polygons (a) and the end month for each subregion (b). The LWY starts from the month with the lowest average monthly streamflow. Colors represent the end months.

csv, “notes.highest” column), seven subregions labeled as “local\_sites\_based”, and 17 subregions labeled “ND\_interpolation” (without streamflow data).

### Technical validation

We assessed the performance of the spatial interpolation method using a leave-one-out cross-validation approach (Sanabria et al. 2013). Firstly, we randomly chose a site

(i.e., river gaging station) and removed its LWY data from the dataset. Then, we applied the ordinary kriging method described above to the new dataset, re-estimated the LWY end month of the removed site, and compared the new estimated LWY end month value with the actual end month. We repeated this process 10 times on 10 different, spatially-separated sites. For both LWY definitions, we found that the estimated and the actual end month of these 10 sites were either the same or differed by 1 month (mean absolute

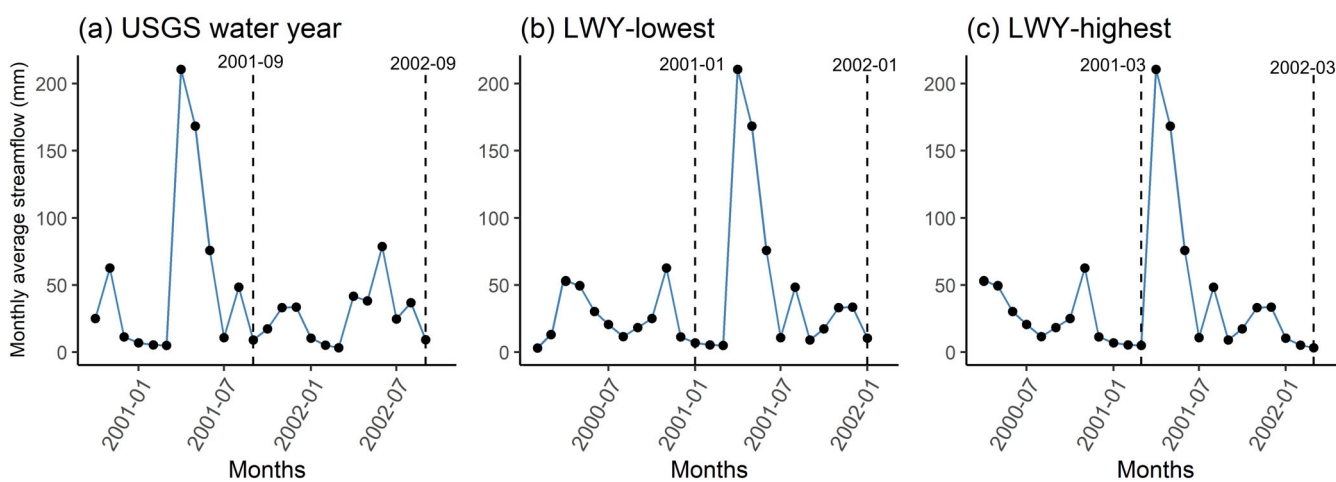


**Fig. 5.** Monthly average streamflow data of Little Fork River (Minnesota, USA, latitude = 48.3958, longitude = -93.5493) in the water years 2001 and 2002 using three LWY definitions: Oct 1<sup>st</sup>–Sep 30<sup>th</sup> water year (sensu USGS) (a), LWY-lowest (b), and LWY-highest (c). The dashed lines indicate the end month of the water years.

difference = 0.4 months for LWY-lowest and 0.5 months for LWY-highest), depending on the streamflow data density of the subregion. Subregions with a higher data density had higher accuracies than areas with a lower density of data.

### Data use and recommendations for reuse

This LWY dataset is intended to provide localized, continental-scale water year timeframes that can be used for studying the features and impacts of precipitation and hydrology across the CONUS. It is important to note that precipitation and hydrological dynamics and patterns can vary by the water year definition (e.g., Fig. 5). Using the Little Fork River in Minnesota (USA) as an example, if a researcher was studying the peak streamflow in April 2001, it would be in water year 2002 when using either LWY-lowest or LWY-highest, but in water

year 2001 when using the water year created by USGS (Oct 1<sup>st</sup>–Sep 30<sup>th</sup>). Thus, it is crucial to choose a water year definition that matches the context and research question being asked. The LWY-lowest can be useful for studying the relationship between precipitation and runoff and local long-term hydrological cycles (e.g., water replenishment and depletion cycle). The LWY-highest can provide more relevant insights for research focused on dry or low-flow periods because it covers the entire low-streamflow period. Finally, in some cases, an alternative definition could be more useful. For example, the USGS water year definition that starts from October 1<sup>st</sup> might be appropriate for hydrological studies in snow-dominated regions.

Here, we provide an example of using these three different timeframes to identify the water years with the lowest and highest annual average streamflow from water years 1991–2018. We assigned each of the 875 sites two LWY end months

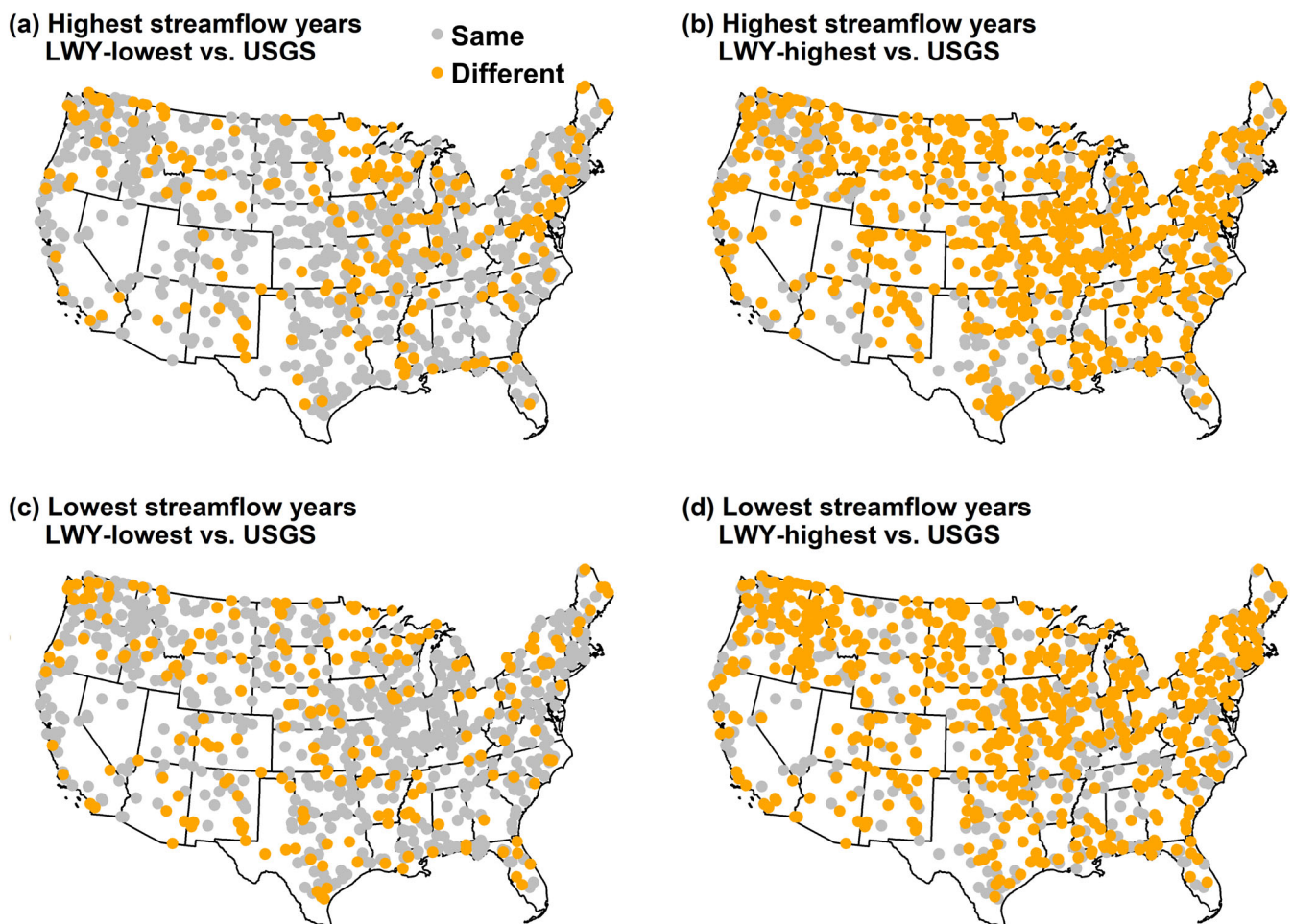


**Fig. 6.** Maps showing the comparison of the highest/lowest streamflow water years across the three water year definitions. Plots (a) and (b) show whether the year with the highest streamflow was the same or different for each site when using different water year definitions. Plot (a) compares LWY-lowest with the Oct–Sep (USGS) water year definition, while plot (b) compares LWY-highest with the Oct–Sep water year. Plots (c) and (d) show whether the year with the lowest streamflow was the same or different for each site when using different water year definitions. Plot (c) compares LWY-lowest with the Oct–Sep water year definition, while plot (d) compares LWY-highest with the Oct–Sep water year. Gray dots indicate that the years were the same between the definitions, and orange dots indicate that the years were different.

(LWY-lowest and LWY-highest) according to the subregion they are located in (i.e., all the sites in the same subregion share the same end month; Sun and Cheruvellil 2024), calculated the annual average streamflows of each site based on these two LWY timeframes, and then determined the water years with the highest and lowest streamflow for each site and timeframe. Then, we calculated the site-specific annual average streamflow based on the water year that ends on September 30<sup>th</sup> (USGS) and determined the water years with the highest and lowest streamflow for each site using that definition of water year. Finally, we compared the highest and lowest streamflow water years between LWY-lowest and the Oct–Sep water year (by USGS) and between LWY-highest and the Oct–Sep water year (by USGS). For all the three definitions, the water year was named by the calendar year in which it ended (e.g., the 12-month period from August 1<sup>st</sup>, 2010 to July 31<sup>st</sup>, 2011 = LWY 2011). We found that, for some sites across the CONUS, the water years with the lowest and highest annual average streamflow were consistent across water year definitions, while for others, these years varied (Fig. 6). Additionally, the comparison between LWY-highest and USGS Oct–Sep water year definition resulted in more sites with different highest and lowest streamflow years (Fig. 6b,d; 75% and 68% were different for the highest and lowest streamflow years, respectively) than the comparison between LWY-lowest and Oct–Sep water year created by USGS (Fig. 6a,c; 25% and 24% for the highest and lowest streamflow years, respectively). These results suggest that the water year definition can influence the identification of extreme streamflow events and highlight the importance of selecting appropriate definitions.

This LWY dataset considers areal variations and can be used in various meteorological, hydrological, and ecological studies to identify and predict trends in precipitation, extreme events (drought and flooding), and water fluxes as well as investigate their effects on ecosystems (e.g., Kamps and Heilman 2018) and human communities (e.g., calculating hydropower generation capacity; Bongio et al. 2016). Future users of the subregion-specific LWYs can combine these data with a wide range of climatic, as well as terrestrial and aquatic abiotic and biotic data, by linking our dataset with other data products, such as LAGOS-US modules (e.g., Cheruvellil et al. 2021) or USGS datasets (e.g., Blodgett 2023) using subregion identifiers (i.e., HU4 codes). Moreover, our R code is available for download at the EDI repository so that users can apply a similar method to other regions around the world to generate site or region-specific LWY timeframes. As such, these data will be a valuable addition to the literature that can contribute to building macroscale understanding of precipitation and streamflow variability and their influences on a variety of systems.

### Author Contributions

Xinyu Sun and Kendra Spence Cheruvellil conceived the project and designed the overall approach. Xinyu Sun

collected and processed the data, wrote the code, and conducted the spatial interpolation. Xinyu Sun wrote the first draft of the manuscript and both authors reviewed and revised the manuscript.

### Acknowledgments

We thank Conrad Wasko and his colleagues for kindly guiding us on how to download data from GRDC and sharing data with us. This work was supported by the U.S. National Science Foundation (NSF) Macrosystems Biology & NEON-Enabled Science Program (DEB 1638679).

### Conflicts of Interest

None declared.

### References

- Augustine, D. J. 2010. “Spatial Versus Temporal Variation in Precipitation in a Semiarid Ecosystem.” *Landscape Ecology* 25, no. 6: 913–925. <https://doi.org/10.1007/s10980-010-9469-y>.
- Blodgett, D. L. 2023. *Twelve-Digit Hydrologic Unit Soil Moisture, Recharge, Actual Evapotranspiration, and Snowpack Water Equivalent Storage From the National Hydrologic Model Infrastructure With the Precipitation-Runoff Modeling System 1980–2016* <https://doi.org/10.5066/P9W148A1>.
- Bongio, M., F. Avanzi, and C. De Michele. 2016. “Hydroelectric Power Generation in an Alpine Basin: Future Water-Energy Scenarios in a Run-Of-The-River Plant.” *Advances in Water Resources* 94: 318–331. <https://doi.org/10.1016/j.advwatres.2016.05.017>.
- Boudibi, S., B. Sakaa, and A. J. Zapata-Sierra. 2019. “Groundwater Quality Assessment Using GIS, Ordinary Kriging and WQI in an Arid Area.” *PONTE International Scientific Research Journal* 75, no. 12: 204–226. <https://doi.org/10.21506/j.ponte.2019.12.14>.
- Brunner, M. I., and L. J. Slater. 2022. “Extreme Floods in Europe: Going Beyond Observations Using Reforecast Ensemble Pooling.” *Hydrology and Earth System Sciences* 26, no. 2: 469–482. <https://doi.org/10.5194/hess-26-469-2022>.
- Caruso, B. S. 2000. “Evaluation of Low-Flow Frequency Analysis Methods.” *Journal of Hydrology. New Zealand* 39, no. 1: 19–47. <https://www.jstor.org/stable/43944831>.
- Chagas, V. B. P., P. L. B. Chaffe, and G. Blöschl. 2024. “Regional Low Flow Hydrology: Model Development and Evaluation.” *Water Resources Research* 60, no. 2: e2023WR035063. <https://doi.org/10.1029/2023WR035063>.
- Cheruvellil, K. S., P. A. Soranno, I. M. McCullough, K. E. Webster, L. K. Rodriguez, and N. J. Smith. 2021. “LAGOS-US LOCUS v1.0: Data Module of Location, Identifiers, and Physical Characteristics of Lakes and Their Watersheds in the Conterminous U.S.” *Limnology and Oceanography Letters* 6, no. 5: 270–292. <https://doi.org/10.1002/lol2.10203>.

- Condon, L. E., and R. M. Maxwell. 2015. "Evaluating the Relationship Between Topography and Groundwater Using Outputs From a Continental-Scale Integrated Hydrology Model." *Water Resources Research* 51, no. 8: 6602–6621. <https://doi.org/10.1002/2014WR016774>.
- Easterling, D. R., G. A. Meehl, C. Parmesan, S. A. Changnon, T. R. Karl, and L. O. Mearns. 2000. "Climate Extremes: Observations, Modeling, and Impacts." *Science* 289, no. 5487: 2068–2074. <https://doi.org/10.1126/science.289.5487.2068>.
- Floriancic, M. G., W. R. Berghuijs, P. Molnar, and J. W. Kirchner. 2021. "Seasonality and Drivers of Low Flows Across Europe and the United States." *Water Resources Research* 57, no. 9: e2019WR026928. <https://doi.org/10.1029/2019WR026928>.
- Gimond, M. 2023. *Intro to GIS and Spatial Analysis*. <https://mgimond.github.io/Spatial/index.html>.
- GRDC. 2023. *GRDC—The Global Runoff Data Centre*. [https://grdc.bafg.de/GRDC/EN/Home/homepage\\_node.html](https://grdc.bafg.de/GRDC/EN/Home/homepage_node.html).
- Grimm, A. M., and A. A. Natori. 2006. "Climate Change and Interannual Variability of Precipitation in South America." *Geophysical Research Letters* 33, no. 19: 2006GL026821. <https://doi.org/10.1029/2006GL026821>.
- Heffernan, J. B., P. A. Soranno, M. J. Angilletta, et al. 2014. "Macrosystems Ecology: Understanding Ecological Patterns and Processes at Continental Scales." *Frontiers in Ecology and the Environment* 12, no. 1: 5–14. <https://doi.org/10.1890/130017>.
- Henshaw, F. F., G. C. Baldwin, G. C. Stevens, and E. S. Fuller. 1915. *Surface Water Supply of the United States, 1911 (Water Supply Paper)*. Washington, DC: U.S. Geological Survey. <https://doi.org/10.3133/wsp312>.
- Hijmans, R. J., J. van Etten, M. Sumner, et al. 2023. *raster: Geographic Data Analysis and Modeling (3.6-23)*. <https://cran.r-project.org/web/packages/raster/index.html>.
- Hong, Y., R. F. Adler, F. Hossain, S. Curtis, and G. J. Huffman. 2007. "A First Approach to Global Runoff Simulation Using Satellite Rainfall Estimation." *Water Resources Research* 43, no. 8: 2006WR005739. <https://doi.org/10.1029/2006WR005739>.
- Intergovernmental Panel On Climate Change. 2021. *Climate Change 2021—The Physical Science Basis: Working Group I Contribution to the Sixth Assessment Report of the Intergovernmental Panel on Climate Change*. Cambridge: Cambridge University Press. <https://doi.org/10.1017/9781009157896>.
- Kamps, R. H., and J. L. Heilman. 2018. "A Method to Calculate a Locally Relevant Water Year for Ecohydrological Studies Using Eddy Covariance Data." *Ecohydrology* 11, no. 7: e1980. <https://doi.org/10.1002/eco.1980>.
- Kundzewicz, Z. W., J. Huang, I. Pinskiar, B. Su, M. Szwed, and T. Jiang. 2020. "Climate Variability and Floods in China—A Review." *Earth-Science Reviews* 211: 103434. <https://doi.org/10.1016/j.earscirev.2020.103434>.
- LaRue, E. A., J. Rohr, J. Knott, et al. 2021. "The Evolution of Macrosystems Biology." *Frontiers in Ecology and the Environment* 19, no. 1: 11–19. <https://doi.org/10.1002/fee.2288>.
- Li, J., and A. D. Heap. 2011. "A Review of Comparative Studies of Spatial Interpolation Methods in Environmental Sciences: Performance and Impact Factors." *Ecological Informatics* 6, no. 3–4: 228–241. <https://doi.org/10.1016/j.ecoinf.2010.12.003>.
- Li, L., J. Sun, H. Wang, et al. 2023. "Spatial Distribution and Temporal Trends of Dietary Niacin Intake in Chinese Residents  $\geq 5$  Years of Age Between 1991 and 2018." *Nutrients* 15, no. 3: 638. <https://doi.org/10.3390/nu15030638>.
- Mock, C. J. 1996. "Climatic Controls and Spatial Variations of Precipitation in the Western United States." *Journal of Climate* 9, no. 5: 1111–1125. [https://doi.org/10.1175/1520-0442\(1996\)009<1111:CCASVO>2.0.CO;2](https://doi.org/10.1175/1520-0442(1996)009<1111:CCASVO>2.0.CO;2).
- Nicotina, L., E. Alessi Celegon, A. Rinaldo, and M. Marani. 2008. "On the Impact of Rainfall Patterns on the Hydrologic Response." *Water Resources Research* 44, no. 12: 2007WR006654. <https://doi.org/10.1029/2007WR006654>.
- Olson, D. M., T. J. Griffis, A. Noormets, R. Kolka, and J. Chen. 2013. "Interannual, Seasonal, and Retrospective Analysis of the Methane and Carbon Dioxide Budgets of a Temperate Peatland." *Journal of Geophysical Research: Biogeosciences* 118, no. 1: 226–238. <https://doi.org/10.1002/jgrg.20031>.
- Pebesma, E., and B. Graeler. 2023. *gstat: Spatial and Spatio-Temporal Geostatistical Modelling, Prediction and Simulation (2.1-1)*. <https://github.com/r-spatial/gstat/>.
- Pike, J. G. 1964. "The Estimation of Annual Run-off from Meteorological Data in a Tropical Climate." *Journal of Hydrology* 2, no. 2: 116–123. [https://doi.org/10.1016/0022-1694\(64\)90022-8](https://doi.org/10.1016/0022-1694(64)90022-8).
- Prein, A. F., G. J. Holland, R. M. Rasmussen, M. P. Clark, and M. R. Tye. 2016. "Running Dry: The U.S. Southwest's Drift into a Drier Climate State." *Geophysical Research Letters* 43, no. 3: 1272–1279. <https://doi.org/10.1002/2015GL066727>.
- R Core Team. 2024. *R: A Language and Environment for Statistical Computing*. Vienna: R Foundation for Statistical Computing. <https://www.r-project.org/>.
- Rose, K. C., R. A. Graves, W. D. Hansen, et al. 2017. "Historical Foundations and Future Directions in Macrosystems Ecology." *Ecology Letters* 20, no. 2: 147–157. <https://doi.org/10.1111/ele.12717>.
- Sanabria, L. A., X. Qin, J. Li, R. P. Cechet, and C. Lucas. 2013. "Spatial Interpolation of McArthur's Forest Fire Danger Index across Australia: Observational Study." *Environmental Modelling & Software* 50: 37–50. <https://doi.org/10.1016/j.envsoft.2013.08.012>.
- Seaber, P. R., F. P. Kapinos, and G. L. Knapp. 2007. *Hydrologic Unit Maps*. U.S. Geological Survey. <https://pubs.usgs.gov/wsp/wsp2294/>.

- Sun, X., and K. S. Cheruvellil. 2024. *Local Water Years for 4-Digit Hydrologic Unit Areas Across the Conterminous United States*. Environmental Data Initiative. <https://portal.edirepository.org/nis/mapbrowse?packageid=edi.1547.3>. <https://doi.org/10.1109/ichi61247.2024.00074>.
- Torre Zaffaroni, P., G. Baldi, M. Texeira, C. M. Di Bella, and E. G. Jobbágy. 2023. "The Timing of Global Floods and its Association with Climate and Topography." *Water Resources Research* 59, no. 7: e2022WR032968. <https://doi.org/10.1029/2022WR032968>.
- USGS. 2024. *Water Resources of the United States: Hydrologic Unit Maps*. <https://water.usgs.gov/gis/huc.html>. <https://water.usgs.gov/GIS/huc.html>.
- Wasko, C., R. Nathan, and M. C. Peel. 2020. "Trends in Global Flood and Streamflow Timing Based on Local Water Year." *Water Resources Research* 56, no. 8: e2020WR027233. <https://doi.org/10.1029/2020WR027233>.
- Wasko, C., R. Nathan, L. Stein, and D. O'Shea. 2021. "Evidence of Shorter more Extreme Rainfalls and Increased Flood Variability under Climate Change." *Journal of Hydrology* 603: 126994. <https://doi.org/10.1016/j.jhydrol.2021.126994>.

Submitted 25 May 2024

Revised 20 February 2025

Accepted 17 May 2025